Reconstruction Quality of Congested Freeway Traffic Patterns Based on Kerner's Three-Phase Traffic Theory

Jochen Palmer
Daimler AG
GR/PTA - HPC: 050-G021
D-71059 Sindelfingen, Germany
Email: jochen.palmer@daimler.com

Hubert Rehborn
Daimler AG
GR/PTF - HPC: 050-G021
D-71059 Sindelfingen, Germany
Email: hubert.rehborn@daimler.com

Iván Gruttadauria
UTN-FRVM
Av. Universidad 450
X5900HLR Villa Maria, Argentine
Email: igruttadauria@frvm.utn.edu.ar

***Abstract*—This paper discusses the reconstruction quality of spatio-temporal congested freeway traffic patterns depending on the information provided by different equipment rates of probe vehicles. In this research Kerner's three-phase traffic theory is applied, which distinguishes two different phases in congested traffic: synchronized flow and wide moving jam. In the presented approach spatio-temporal congested traffic patterns are reconstructed from intelligent probe vehicle information generated by an on-board traffic state detection, identifying traffic states along a vehicle's trajectory at any time. With a data fusion algorithm combining the data of several probe vehicles, a detailed picture of spatio-temporal congested traffic patterns is revealed. Comparing *Ground-Truth* with the reconstructed traffic pattern shows that a reconstruction quality comparable to that of established traffic flow models is achievable with probe vehicle equipment rates of about 0.5 %. At higher equipment rates of about 1-1.5 % the achievable quality already exceeds the quality established traffic flow models are able to offer based on a dense detector network with average detector distances of 1-2 km.**

Keywords-Traffic monitoring; Traffic state detection; Traffic data fusion; Probe vehicle data; Three-phase traffic theory; Models ASDA and FOTO; Traffic data quality; Traffic quality indices.

I. Introduction

Nowadays, congested traffic on highways is still a major problem with severe implications for personal life and the economy. In recent years, congested traffic data was mostly gathered with stationary loop detectors. It is expensive to equip a road network with detectors of high quality and small detector distance. Recent progress in mobile communication technology, like WLAN and 3G/UMTS, allows traffic data to be gathered by probe vehicles. In this research the question is answered how many probe vehicles are needed to deliver a quality of traffic data comparable to a dense high quality detector network.

In order to assess the quality of reconstructed traffic patterns, three different quality indices are introduced and assessed. In [16] some basic results have been already presented for the quality index for travel time and the quality index for regions of synchronized flow and wide moving jams. The quality index for fronts of synchronized flow and wide moving jams has been briefly introduced but not evaluated. The other two quality indices have been evaluated based on a congested traffic situation representing a general pattern (GP) according to Kerner's Three Phase Traffic Theory. General patterns occur when there is just a single effective bottleneck. Hence the emerging spatio-temporal patterns are fairly simple.

In this research based on [16] a more detailed assessment of the reconstruction quality is conducted based on an extended traffic situation. The examined situation represents an expanded pattern (EP) according to Kerner's Three Phase Traffic Theory. In this situation traffic patterns emerging at several adjacent effective bottlenecks are overlapping. Hence the resulting combined spatio-temporal traffic patterns show a very complex structure and dynamics. In addition, for the first time, a thorough assessment of the quality index for fronts of synchronized flow and wide moving jams is presented. This allows a detailed discussion of the achievable quality of probe vehicle based models in comparison to stationary loop detector based systems. This research takes all quality aspects of spatio-temporal congested freeway patterns, covered by the three three presented quality indices, into consideration.

Outline

The paper starts with a brief introduction to Kerner's Three Phase Traffic Theory. Basic elements as well spatio-temporal traffic patterns are explained. The traffic models ASDA (Automatische Staudynamikanalyse; automatic congestion analysis) and FOTO (Forecasting of Traffic Objects) based on this theory are described. They reconstruct congested traffic patterns from data measured by stationary loop detectors.

After that the impact of spatio-temporal traffic pattern on vehicles moving through these patterns is discussed.

New methods, which allow the reconstruction of spatio-temporal traffic patterns from data measured by probe vehicles, are briefly introduced. This approach allows a high quality reconstruction of traffic patterns in the whole traffic network without having to rely on stationary loop detectors.

Then three quality indices are introduced and discussed in detail. This includes quality indices for (i) travel time, (ii) fronts of synchronized flow and wide moving jams as well as (iii) regions of synchronized flow and wide moving jams. These quality indices allow the assessment of the reconstruction quality on spatio-temporal traffic patterns. An approach to the simulation of a realistic test dataset is presented.

Based on this dataset and the presented quality indices, the reconstruction quality of the new methods is compared to the reconstruction quality of the traffic models ASDA and FOTO.

II. Kerner's Three Phase Traffic Theory

Based on extensive traffic data analyses of available stationary detector measurements spanning several years Kerner discovered that in addition to free flow (F) two different traffic phases must be differentiated in congested freeway traffic: synchronized flow (S) and wide moving jam (J) ([5], [8]).

A. Elements of Three Phase Traffic Theory

Empirical macroscopic spatio-temporal objective criteria for traffic phases as elements of Kerner's three-phase traffic theory ([5], [8]) are as follows:

1) A wide moving jam is a moving jam that maintains the mean velocity of the downstream jam front, even when the jam propagates through any other traffic state or freeway bottleneck.
2) In contrast, the downstream front of the synchronized flow phase is often fixed at a freeway bottleneck and does not show the characteristic features of wide moving jams.

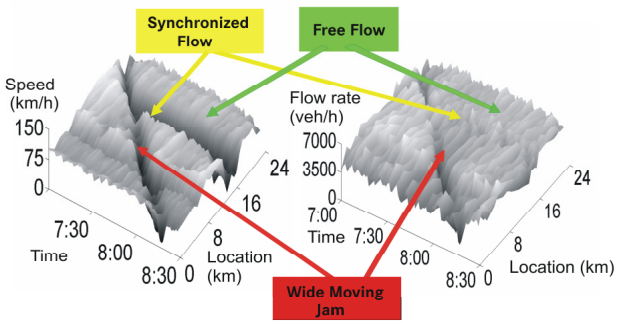

Figure 1. Explanation of traffic phase definitions from empirical data: Spatio-temporal overview of speed (left) and flow rate of traffic (right) on a selected freeway section

However, neither the observation of speed synchronization in congested traffic nor other relationships and features of congested traffic measured at specific freeway locations (e.g., in the flow-density plane) are a criterion for the phase differentiation. The clear differentiation between the synchronized flow and wide moving jam phases can be made on the above objective criteria 1) and 2) only.

Figure 1 illustrates a vehicle speed and flow profile over time and space based upon real measured traffic data. A wide moving jam propagates upstream as a *low speed valley* through the freeway stretch. In contrast, a second speed valley is fixed at the bottleneck location: this congested traffic phase belongs to the synchronized flow phase.

B. Spatio-Temporal Congested Traffic Patterns

The distribution of traffic phases over time and space on a road represents a spatio-temporal congested traffic pattern. Kerner's three-phase traffic theory is able to explain all empirically measured traffic patterns on various roads in many different countries ([19], [20]).

C. Models ASDA and FOTO

For recognition, tracking and prediction of the spatio-temporal congested traffic patterns, based on stationary loop detectors, the models ASDA and FOTO ([5], [8]) have been proposed by Kerner based on the key elements of the theory. Nowadays, the models ASDA and FOTO are deployed in the federal state of Hessen and in the free state of Bavaria where they perform online processing of data [9]. In addition they have been successfully used in a laboratory environment on the M42 near Birmingham, UK and the I-405 in California, USA (Figure 2). In recent years other models, which are similar to the models ASDA and FOTO, have also been published [22].

III. Impacts for Vehicles and Vehicular Assistance Application

Vehicles driving through a spatio-temporal congested traffic pattern experience a number of traffic state changes. A traffic state change represents a unique and exact position in time and space where the traffic phase changes, e.g., from free flow to wide moving jam. It is experienced at any position, where a vehicle hits the upstream or downstream front of a region of a traffic phase. In contrast a traffic phase transition represents the start point or the end point, respectively, of a traffic phase and occurs only twice for each region of a traffic phase (see Figure 3).

Traffic state changes between the different traffic phases have impacts of different strength on the vehicle and vehicular assistance applications [2]. Two of the most distinguishing parameters of different traffic phases from a vehicle's perspective are the vehicle speed v and the vehicle density ρ. Both parameters influence the ability of the vehicles to choose their driving speed as well as the possibility for them to overtake other vehicles and to freely choose their driving lane. Different traffic state changes have a different effect on the value of these parameters. Table I and Table II show the expected changes for the possible speed v and the vehicle density ρ, respectively.

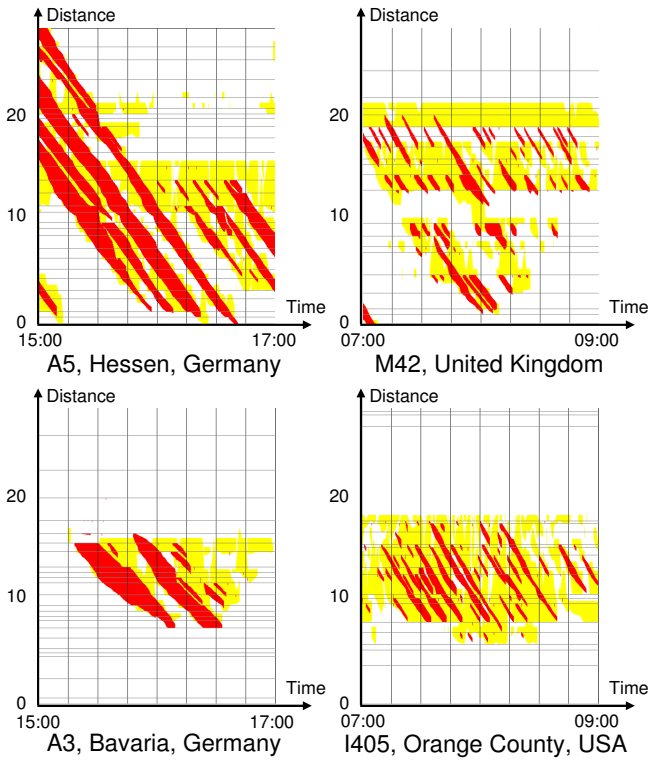

Figure 2. Resulting empirical spatio-temporal traffic patterns when applying the models ASDA and FOTO to traffic data measured in different countries [15]. All these patterns show the same spatio-temporal structure and dynamics: Regions of synchronized flow fixed at the location of the bottleneck and wide moving jams propagating upstream with constant speed.

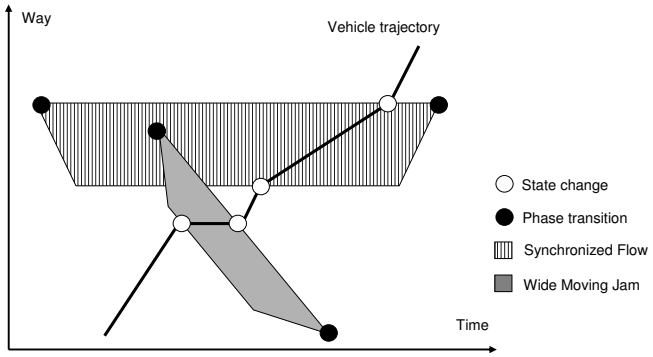

Figure 3. Qualitative explanation of traffic phase transitions and traffic state changes a vehicle experiences on its way through a spatio-temporal congested traffic pattern

Table I
VEHICLE SPEED: CHANGE DEPENDING ON SPECIFIC TRAFFIC STATE TRANSITIONS

State	to F	to S	to J
F	-	Deceleration	Strong deceleration
S	Acceleration	-	Deceleration
J	Strong acceleration	Acceleration	-

Table II
VEHICLE DENSITY: CHANGE DEPENDING ON SPECIFIC TRAFFIC STATE TRANSITIONS

State	to F	to S	to J
F	-	Increase	Strong increase
S	Decrease	-	Increase
J	Strong decrease	Decrease	-

Vehicular assistance applications, like adaptive cruise control or hybrid engine control depend on and benefit from the knowledge of the current and in some cases future values of these parameters ([7], [11]). Each traffic state change represents a control and parameter adaption point for these applications. The better the reconstruction of the spatio-temporal structure of congested traffic patterns, the better the knowledge about current and future spatio-temporal positions of traffic state changes and hence the higher the potential of improving the open- and closed-loop control of vehicular assistance applications. Having a high quality knowledge about current and future traffic state changes opens the door for a complete new class of vehicular assistance applications:

- Safety related systems: Vehicular assistance applications, which improve vehicle safety by being aware of sudden speed breakdowns on the path of a vehicle, for example caused by traffic state changes from phase F to phase J.
- Energy efficient systems: Vehicular assistance applications, which improve the energy efficiency of vehicles by reducing fuel consumption by being aware of current and future traffic states.

In addition a high quality reconstruction of spatio-temporal traffic patterns allows the application of existing vehicular assistance applications in better quality. For example a better knowledge of the travel time loss caused by spatio-temporal congested traffic patterns improves the quality of existing dynamic route guidance systems.

IV. RECONSTRUCTION OF SPATIO-TEMPORAL CONGESTED TRAFFIC PATTERNS

A. Traffic State Detection in Autonomous Vehicle

Instead of stationary loop detectors, probe vehicle data is used for the detection and reconstruction of spatio-temporal congested traffic patterns. Many systems using probes transmit only aggregated travel times for pre-defined road sections [4]. Here, we are not only interested in the travel time losses caused by spatio-temporal congested traffic patterns, but also in their detailed structure (Figure 3, [5], [8]).

In Kerner's three-phase traffic theory there is one phase of free flow (F) and two phases of congested traffic, synchronized flow (S) and wide moving jam (J). Each traffic pattern consists of a unique formation and behavior of regions in

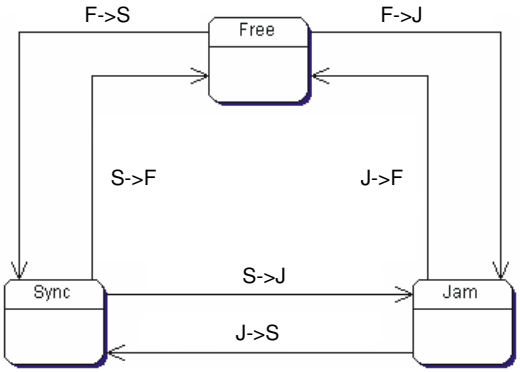

Figure 4. State diagram for three traffic phases [6]

time and space belonging to exactly one of these three phases. One of these three phases is assigned to each of the probe positions in time and space in an autonomous way ([6], [8]). A traffic state change is performed when the chosen measured values are above or below specific thresholds in speed and time, which are chosen according to on-board traffic criteria [10].

B. Cooperative Reconstruction of Traffic Patterns

For the reconstruction of spatio-temporal congested traffic patterns a clustering algorithm is employed. First, the traffic phase is identified, then depending on the identified traffic phase, an algorithm tailored for the specific characteristic features of the synchronized flow and wide moving jam traffic phases is applied [17] (Figure 5).

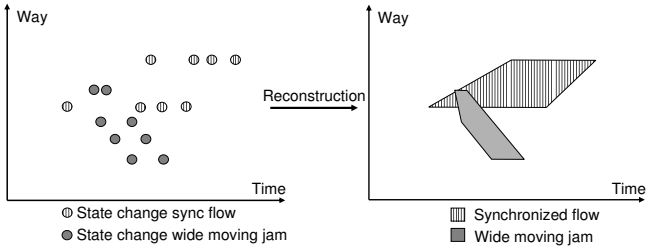

Figure 5. Using clustering to reconstruct traffic patterns from traffic state changes [15]

V. Reconstruction Quality Indices

The reconstruction quality of spatio-temporal congested traffic patterns can only be assessed in the case that the real spatio-temporal traffic pattern is known. Full knowledge about spatio-temporal traffic patterns is only possible, when the positions of all vehicles participating in traffic flow are known for any time instant. This is still difficult to achieve, even with the recent advances in traffic measurement technology. Hence any measured traffic pattern, which represents the *best-known* information about a real traffic pattern, exhibits *some* deviation to reality. The best known traffic information is called *Ground-Truth*. Therefore, when the quality of reconstructed spatio-temporal congested traffic patterns is assessed by comparing them to *any* measured *Ground-Truth* information about this patterns, it is only possible to assess their error compared to *Ground-Truth*, but not their deviation to reality.

In the following sections a formal definition of spatio-temporal congested traffic patterns is introduced. Based on this definition, three different quality indices are presented: a quality index for travel time, a quality index for fronts of synchronized flow and wide moving jam and a quality index for regions of synchronized flow and wide moving jam. Each of the quality indices assesses a different feature of spatio-temporal congested traffic patterns.

A. Formal Definition of Traffic Patterns

In a continuous traffic reality a traffic state TS is assigned to each spatio-temporal position $P(x,t)$, whereas x represents a continuous value in distance and t a continuous value in time. The traffic reality R represents the combination of all

$$TS(x,t) \in \{F,S,J\} \tag{1}$$

within the spatial borders x_s and x_e as well as the temporal borders and t_s and t_e, hence

$$R := \{TS(x,t) | x_s \leq x \leq x_e \wedge t_s \leq t \leq t_e\} \tag{2}$$

Compared to R a reconstruction of traffic patterns using a model M in most cases shows deviations in time and space. The quality Q of the reconstruction is given by the deviation D between M and R. Hence

$$M := \{TS(x,t) | x_s \leq x \leq x_e \wedge t_s \leq t \leq t_e\} \tag{3}$$

$$Q = D_{M \to R} \tag{4}$$

As mentioned above, currently it is difficult to measure traffic reality. In addition storing and processing continuous spatio-temporal information is not feasible. For example, when stationary loop detectors are used to measure traffic reality, the continuous values of time and distance are actually measured as discrete values. These values average time and distance in discrete intervals.

Consequently, x and t degrade to the discrete values x_d and t_d. Their resolution represents the quality of knowledge about the spatio-temporal information. In common systems using stationary loop detectors the temporal resolution is in most cases $t_d = 1$ min, while the spatial resolution is in the best case $x_d = 1-2$ km. In many cases the spatial resolution is even lower. This means that the traffic reality is known with even less quality.

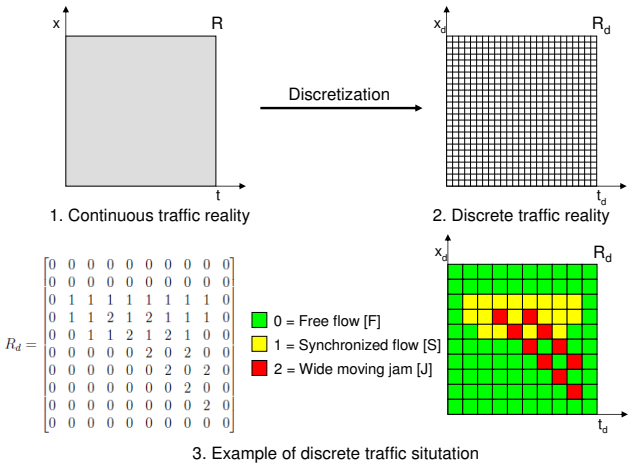

Figure 6. Discretization of spatio-temporal congested traffic patterns

Using x_d and t_d the continuous traffic reality R becomes the discrete traffic reality R_d as shown in Figure 6. By taking the border spatial borders x_s and x_e and the temporal borders t_s and t_e into account, R_d represent information about a traffic pattern TP_{R_d} within some spatio-temporal boundary:

$$TP_{R_d} := \{TS_d(x,t) | x_s \leq x_0, x_1 ... x_n \leq x_e \wedge t_s \leq t_0, t_1 ... t_n \leq t_e\} \quad (5)$$

In order to determine the discrete quality Q_d, a discrete model output M_d with the same spatial and temporal resolutions x_d and t_d is required. This model represents the reconstructed traffic pattern TP_M:

$$TP_M := \{TS_d(x,t) | x_s \leq x_0, x_1 ... x_n \leq x_e \wedge t_s \leq t_0, t_1 ... t_n \leq t_e\} \quad (6)$$

For Q_d this leads to

$$Q_d = D_{TP_M \rightarrow TP_{R_d}} \quad (7)$$

B. Quality Index for Travel Time

For each point in time t the total travel time T_{total} consisting of free flow travel time and congested travel time can be calculated as shown in [18]

$$T_{total}(t) = \frac{L_F(t)}{v_F(t)} + \frac{L_J(t)}{v_J(t)} + \frac{L_S(t)}{v_S(t)} \quad (8)$$

where $L_F(t)$, $L_S(t)$ and $L_J(t)$ represent the lengths of the traffic phases and $v_F(t)$, $v_S(t)$ and $v_J(t)$ represent the average speeds within these phases at time t.

The travel time $T_{total}(t)$ can be determined for road segment based on a reconstructed traffic pattern TP_M and based on a traffic pattern TP_{R_d}, which has been defined as *Ground-Truth*. In this case the travel time through the reconstructed traffic pattern is represented by T_M and the travel time through *Ground-Truth* is defined as T_{GT}. By calculating the relative average deviation ΔT between T_M and T_{GT}, is is possible to assess the quality index for travel time for a given spatio-temporal region [14]. The assessment takes spatio-temporal regions between the spatial border x_s and x_e on N time instants between the temporal boundaries t_s and t_e into account:

$$\Delta T = \frac{1}{N} \sum_{t=t_s}^{t_e} \frac{|T_M(t) - T_{GT}(t)|}{T_{GT}(t)} \quad (9)$$

The quality index given by (9) is represented by a number $\Delta T \geq 0$. A result of $\Delta T = 0$ represents the best possible quality, which is achieved, when T_M and T_{GT} are the same for all time instants t.

C. Quality Index for Fronts of S and J

Positions of phase fronts of the traffic phases *S* and *J* are denoted by $x_{up}(t)$ and $x_{down}(t)$ for each time instant t. Hence, expanded spatio-temporal congested traffic patterns can show several phase fronts at a given time t. Phase fronts can be reconstructed based on a reconstructed traffic pattern TP_M or based on a traffic pattern TP_{R_d}, which has been defined as *Ground-Truth*. For each time t and each *phase* the positions of the upstream front are defined as $x_{up_M}^{Phase}(t)$ and $x_{up_{GT}}^{Phase}(t)$, while the positions of the downstream front are designated as $x_{down_M}^{Phase}(t)$ and $x_{down_{GT}}^{Phase}(t)$, respectively. The reconstruction quality of each single phase front is determined by the relative average deviation of both positions at N time instants between the temporal boundaries t_s und t_e.

The quality of an upstream phase front is given by Δ_{up}^{Phase}

$$\Delta_{up}^{Phase} = \frac{1}{N} \sum_{t=t_s}^{t_e} |x_{up_M}^{Phase}(t) - x_{up_{GT}}^{Phase}(t)| \quad (10)$$

while the quality of a downstream phase front is given by Δ_{down}^{Phase}:

$$\Delta_{down}^{Phase} = \frac{1}{N} \sum_{t=t_s}^{t_e} |x_{down_M}^{Phase}(t) - x_{down_{GT}}^{Phase}(t)| \quad (11)$$

Both quality indices give as a result the relative average deviation in meters between a reconstructed phase front and a phase front, which has been defined as *Ground-Truth*. Hence $\Delta_{up}^{Phase} \geq 0\ m$ and $\Delta_{down}^{Phase} \geq 0\ m$. The best quality is achieved, when both phase fronts are the same. This is represented by $\Delta_{up}^{Phase} = 0\ m$ and $\Delta_{down}^{Phase} = 0\ m$.

Within a traffic pattern, which has been defined as *Ground-Truth*, a phase front occurs on $N(GT)$ time instant between the temporal borders t_s and t_e. In this period a single phase front shows no gaps. If it would be the case it would not be a single phase front, but instead *several* phase

fronts. Hence, in addition to the reconstruction quality of a phase front, its coverage is assessed. Coverage is defined as the ratio of $N(M)$ time instants where the phase front was reconstructed by a model with respect to $N(GT)$ time instants where the phase front was present in *Ground-Truth*. This leads to two addition quality indices, which measure the coverage of both the upstream and downstream phase fronts.

The coverage of the upstream phase front is given by C_{up}^{Phase}

$$C_{up}^{Phase} = \frac{N_{up}^{Phase}(M)}{N_{up}^{Phase}(GT)} \tag{12}$$

while C_{down}^{Phase} gives the coverage of the downstream phase front:

$$C_{down}^{Phase} = \frac{N_{down}^{Phase}(M)}{N_{down}^{Phase}(GT)} \tag{13}$$

Both C_{up}^{Phase} and C_{down}^{Phase} give a result between 0 and 1, describing the coverage of a *Ground-Truth* phase front by a reconstructed one. Best coverage is achieved by $C_{up}^{Phase} = 1$ and $C_{down}^{Phase} = 1$.

All quality indices for phase fronts emphasize some specific aspects of a spatio-temporal congested traffic pattern. They assess the quality of the reconstruction of a *specific* phase fronts, hence they do not represent a quality index for *all* phase fronts of a traffic pattern.

D. Quality Index for Regions of S and J

The quality index for regions of *S* and *J* assesses the general reconstruction quality between a traffic pattern TP_M reconstructed by a model M and traffic pattern TP_{GT}, which has been defined as the *Ground-Truth* reference information. For each congested traffic phase the spatio-temporal areas they cover are compared against each other with regard to hits and false alarms. Figure 7 illustrates this concept, representing an adaption of the ROC[1]-analysis for traffic data. The origin of ROC-analysis is medical diagnostics [23]. Since a few years its concepts have also been applied to machine learning [24].

The ROC-analysis is previously been applied for assessing the quality of traffic data [1]. However, in this case only the classes *congested* and *not congested* have been considered [12]. In [16], the ROC-analysis was extended and applied to traffic data containing three distinct traffic phases.

The definitions of TP_M and TP_{R_d} given in the previous section can directly be applied to yield a computationally efficient calculation of this quality index. The *Ground-Truth* reference information use for quality assessment is defined as TP_{GT}. For both TP_M and TP_{GT} three binary matrices are calculated, one for each traffic phase. These matrices

[1]ROC - Receiver operating characteristic

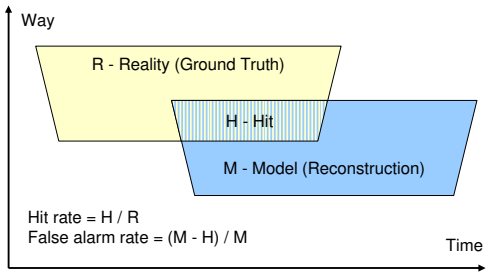

Figure 7. Definition of the Quality Index for Regions of Synchronized Flow and Wide Moving Jam

contain the number 1 at all spatio-temporal positions where a specific traffic phase occurs and the number 0 at all other positions.

For TP_M this leads to TP_M^F, TP_M^S and TP_M^J and for TP_{GT} to TP_{GT}^F, TP_{GT}^S and TP_{GT}^J, respectively. Using a row vector r_v and a column vector c_v with correct dimension for TP_M and TP_{GT} with all $a_{ij} = 1$ allows to count the number c of elements a_{ij} within matrix A where $a_{ij} = 1$.

$$c = r_v * A * c_v \tag{14}$$

The reconstruction quality of spatio-temporal traffic patterns can now be assessed based on ROC-analysis [3] using the ROC measure TPR (true-positive-rate),

$$TPR = \frac{t_p}{t_p + f_n} \tag{15}$$

the measure FPR (false-positive-rate)

$$FPR = \frac{f_p}{t_n + f_p} \tag{16}$$

and finally the measure FAR (false alarm rate)

$$FAR = \frac{f_p}{t_p + f_p} \tag{17}$$

whereas t_p represents the true-positives, f_p the false-positives, t_n the true-negatives and f_n the false-negatives. Figure 8 shows this for a feature space having the features A and B, where the classification of a class G is performed by a classificator C.

This leads to different definitions of t_p, f_p, t_n, f_n and TPR, FPR and FAR for both congested traffic phases *S* and *J*.

1) Traffic phase S*:* For synchronized flow *S* the classification of a traffic state TS at a position P_d results in the following different cases according to ROC definitions:

1) True positive t_p: $TS_M = S \wedge TS_{GT} = S$
2) False positive f_p: $TS_M = S \wedge (TS_{GT} = J \vee TS_{GT} = F)$
3) True negative f_n: $(TS_M = J \vee TS_M = F) \wedge (TS_{GT} = J \vee TS_{GT} = F)$

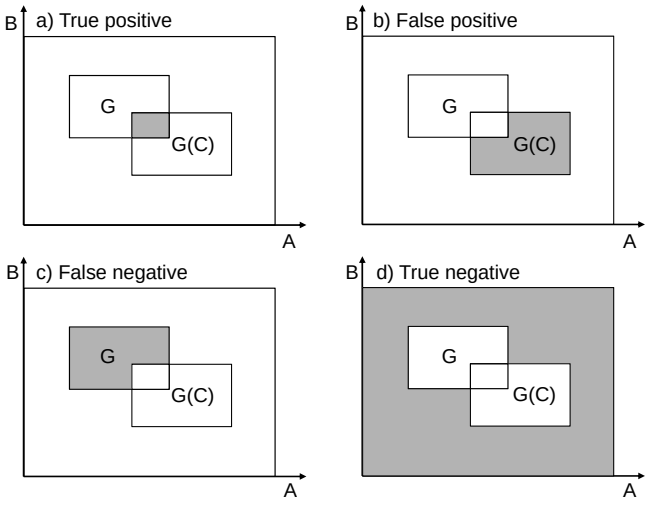

Figure 8. Basic ROC definitions

4) False negative t_n: $(TS_M = J \vee TS_M = F) \wedge TS_{GT} = S$

Taking these definitions into account, the corresponding values for TPR_S, FPR_S and FAR_S are calculated as follows:

$$TPR_S = \frac{z_v * (TP_M^S \wedge TP_{GT}^S) * s_v}{z_v * TP_{GT}^S * s_v} \tag{18}$$

$$FPR_S = \frac{z_v * (TP_M^S \wedge TP_{GT}^J + TP_M^S \wedge TP_{GT}^F) * s_v}{z_v * (TP_{GT}^J + TP_{GT}^F) * s_v} \tag{19}$$

$$FAR_S = \frac{z_v * (TP_M^S \wedge TP_{GT}^J + TP_M^S \wedge TP_{GT}^F) * s_v}{z_v * TP_M^S * s_v} \tag{20}$$

All quality indices TPR_S, FPR_S and FAR_S give values between 0 and 1.

The index TPR_S describes the ratio of TP_{GT}, which is covered by TP_M. A value of $TPR_S = 1$ corresponds to the best possible quality. In this case TP_{GT} is completely covered by TP_M. The worst possible quality is represented by $TPR_S = 1$, when the reconstructed traffic pattern does not cover any region of the real traffic pattern.

In contrast to TPR_S, the index FPR_S describes the ratio of TP_{GT}, which is by mistake classified as traffic phase *S*. Hence the best possible quality corresponds to $FPR_S = 0$, while the worst possible quality corresponds to $FPR_S = 1$.

Finally, the false alarm rate FAR_S describes the ratio of TP_M, which by mistake classifies the traffic phase *S*. The best possible quality corresponds to $FAR_S = 0$, while the worst possible quality corresponds to $FAR_S = 1$.

The special case $TPR_S = 1$, $FPR_S = 0$ and $FAR_S = 0$ represents the best possible quality, when all three indices are taken into account. In this case TP_M and TP_{GT} are completely congruent, the traffic pattern reconstructed by the model is in accordance to real traffic pattern.

2) Traffic phase J*:* For the traffic phase wide moving jam *J* the classification of a traffic state TS at a position P_d results in the following possible cases:

1) True positive r_p: $Z_M = J \wedge Z_{GT} = J$
2) False positive f_p: $Z_M = J \wedge (Z_{GT} = S \vee Z_{GT} = F)$
3) True negative f_n: $(Z_M = S \vee Z_M = F) \wedge (Z_{GT} = S \vee Z_{GT} = F)$
4) False negative r_n: $(Z_M = S \vee Z_M = F) \wedge Z_{GT} = J$

The corresponding values for TPR_J, FPR_J and FAR_J are calculated as follows:

$$TPR_J = \frac{z_v * (TP_M^J \wedge TP_{GT}^J) * s_v}{z_v * TP_{GT}^J * s_v} \tag{21}$$

$$FPR_J = \frac{z_v * (TP_M^J \wedge TP_{GT}^S + TP_M^J \wedge TP_{GT}^F) * s_v}{z_v * (TP_{GT}^S + TP_{GT}^F) * s_v} \tag{22}$$

$$FAR_J = \frac{z_v * (TP_M^J \wedge TP_{GT}^S + TP_M^J \wedge TP_{GT}^F) * s_v}{z_v * TP_M^J * s_v} \tag{23}$$

Again TPR_J, FPR_J and FAR_J give all values between 0 and 1. Regarding maximum and minimum quality they behave like their counterparts for the traffic phase *S*.

E. Summary

Table III gives an overview of all defined quality indices and the values, which represent the maximum and minimum quality.

Table III
OVERVIEW OF ALL DEFINED QUALITY INDICES

Index	Phase	Maximum Quality	Minimum Quality
ΔT	F, S, J	0	∞
Δ_{up}^S	S	0	∞
Δ_{down}^S	S	0	∞
C_{up}^S	S	1	0
C_{down}^S	S	1	0
Δ_{up}^J	J	0	∞
Δ_{down}^J	J	0	∞
C_{up}^J	J	1	0
C_{down}^J	J	1	0
TPR_S	S	1	0
FPR_S	S	0	1
FAR_S	S	0	1
TPR_J	J	1	0
FPR_J	J	0	1
FAR_J	J	0	1

Indices, which relate to a deviation Δ, show the maximum quality, when the deviation is small $\Delta = 0$. Hence the minimum quality is represented by a large deviation $\Delta >> 0$.

The maximum quality of the coverage C is full coverage $C = 1$, while the minimum quality is represented by no coverage $C = 0$.

The indices TPR, FPR and FAR have their maximum quality at a maximum of correct classifications and a minimum of false classifications. Hence the maximum quality is represented by $TPR = 1$, $FPR = 0$ and $FAR = 0$, while the minimum quality is represented by $TPR = 0$, $FPR = 1$ and $FAR = 1$.

VI. Test Environment

The Kerner-Klenov microscopic three-phase traffic model ([5], [8]) has been used for the generation of a large number of single vehicle trajectories. As input data for the model a description of the simulated track as well as initial starting conditions of speed and flow at the most upstream border are required. All other areas in space and time are governed by the Kerner-Klenov model. The microscopic model's output can be regarded as a realization of *Ground-Truth*, which is qualitatively comparable to spatio-temporal congested traffic patterns measured on highways ([5], [8]).

Ground-Truth denotes in this context that the model output represents the reference information or the *reality*, which should be reconstructed by a traffic model using the vehicle trajectories as base data. Quality is therefore measured as the difference between *Ground-Truth* and the cooperative reconstruction of spatio-temporal congested traffic patterns based on the generated trajectories.

First, a traffic state detection is performed in each virtual vehicle, in order to detect all traffic state changes this virtual vehicle experiences. After that all traffic state changes are combined to a reconstructed congested traffic pattern by applying a clustering algorithm. It combines the autonomously detected traffic state changes of several probe vehicles to a collective and cooperatively reconstructed traffic pattern (see Figure 9).

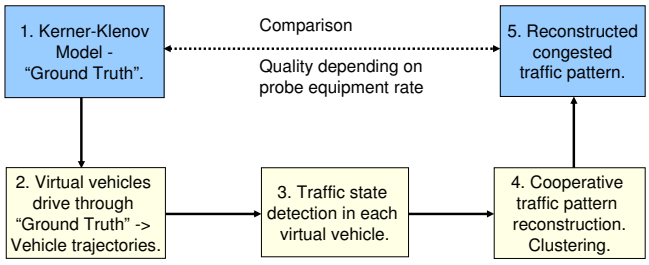

Figure 9. Steps necessary for probe equipment rate investigations

VII. Results

A. Examined Situation

For evaluation the Kerner-Klenov three-phase microscopic model was used to simulate an expanded spatio-temporal congested traffic pattern. The simulation was configured to simulate a 30 km highway stretch with three lanes and three junctions containing on- and off-ramps. The incoming and outgoing flow at these three junctions leads to the realization of three bottlenecks, which could lead to an $F \rightarrow S$ traffic breakdown and the formation of several regions of synchronized flow. Within the synchronized flow regions several wide moving jams emerged (Figure 10).

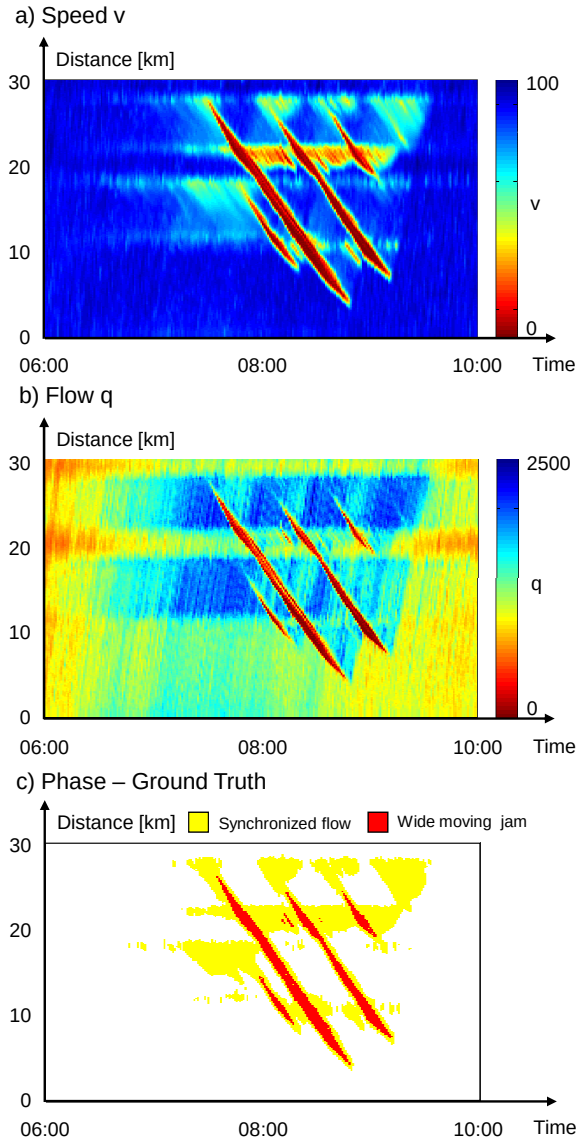

Figure 10. Kerner-Klenov simulation output of an expanded pattern. Average vehicle speed is shown in Figure a), average vehicle flow is shown in Figure b), while Figure c) shows the traffic phase of *Ground-Truth* at a given spatio-temporal position. Wide moving jams can be identified in all three figures as stable structures moving upstream with a constant speed. In contrast the downstream front of the traffic phase synchronized flow is stationary fixed at the location of the bottlenecks.

In the following sections, the quality index results of model using probe vehicle data are compared with the results of the ASDA and FOTO models based on stationary loop

detector data. In order to achieve this, the simulated situation was reconstructed by both the model using probe vehicle data and the ASDA and FOTO models using different configurations of input data. Then the achievable quality was assessed by using the quality indices introduced earlier in this paper.

The models ASDA and FOTO were used with different detector configurations. The average distance ranged between about 1 km until up to up 9 km. Results of the models ASDA and FOTO with two different detector configurations are shown in Figure 11.

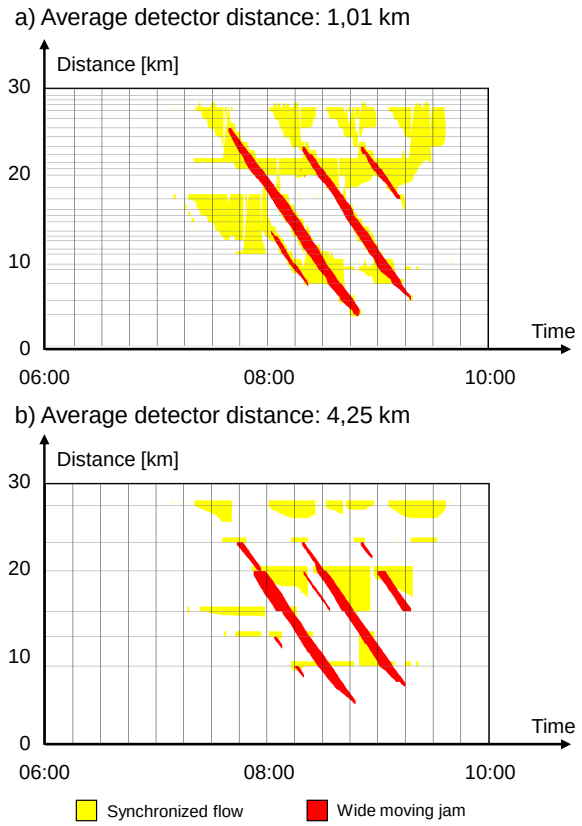

Figure 11. Example results for the models ASDA and FOTO

The traffic models based on probe vehicle data were used with different equipment rates of probe vehicles ranging between 4 % and 0.25 %. Results of the vehicles based models are shown in Figure 12. Each assessed equipment rate was examined based on 100 random distributions of this equipment rate. Each random distribution of a given equipment rate was selected from all vehicles, which are part of the traffic flow. Each selected random distribution represents one possible realization of this equipment rate. By comparing the results of all random distributions of one equipment rate, the influence of different realizations on the achievable results at a given equipment rate can be derived.

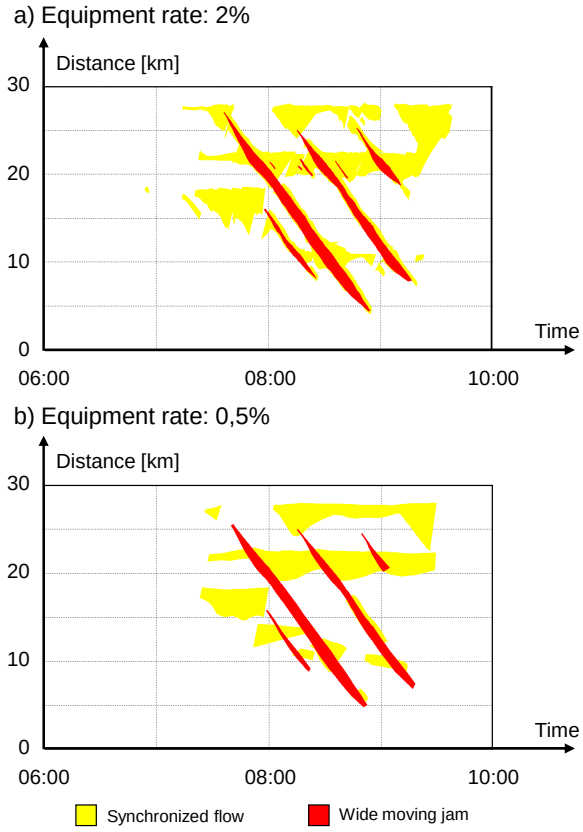

Figure 12. Example results for vehicle based methods

B. *Quality Index for Travel Time*

The results of both models were assessed using the quality index for travel time. Figure 13 shows the results for the ASDA and FOTO models, while Figure 14 shows the results of the model based on probe vehicle data.

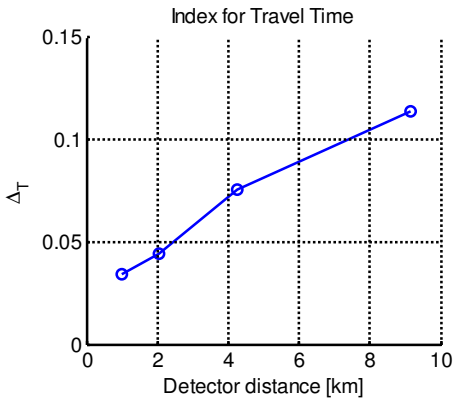

Figure 13. Quality Index for Travel Time: ASDA and FOTO

Using the quality index for travel time the dependence of the model result from the available input data is visible. The probe vehicle based methods generally offer a better quality

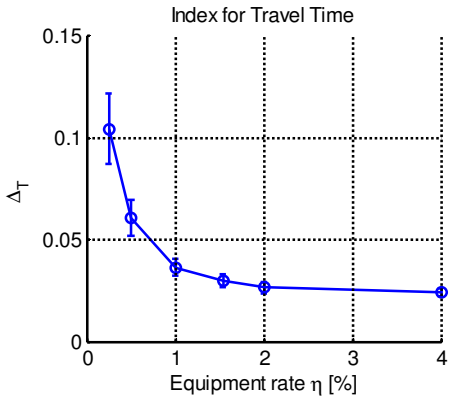

Figure 14. Quality Index for Travel Time: Vehicles

compared to the ADSD/FOTO models. At a equipment rate of about 1 % the achievable results are comparable to a high quality detector network having an average detector distance of 1-2 km.

C. Quality Index for Fronts of Synchronized Flow and Wide Moving Jam

The results of both models were also compared using the quality index for fronts of synchronized flow and wide moving jam. At first the deviation of fronts depending on the input data were examined. Figure 15 shows the results for the models ASDA and FOTO, while Figure 16 shows the results for the models based on probe vehicle data. For both examined jams the models based on probe vehicle data show superior results. At the best detector configuration having an average detector distance of only 1 km the ASDA and FOTO models achieve a front deviation of about 200 m for both jams. This increases up to 300 - 800 m when the average detector distance increases up to over 9 km. The models based on probe vehicle data achieve a front deviation of at most 200 m down to a equipment rate of only 0.5 %. At higher equipment rates the front deviation is even smaller. This corresponds to an even better quality.

After that the front coverage was examined for both models. Figure 17 shows the results for the ASDA and FOTO models. In Figure 18, the results for the models based on probe vehicle data are shown. The quality index for front coverage shows comparable results: the models based on probe vehicle data are superior to the models ASDA and FOTO. Even at an equipment rate of only 1 % the results of the vehicle based models are comparable to ASDA and FOTO used with an average detector distance of only 1 km.

D. Quality Index for Regions of Synchronized Flow and Wide Moving Jam

Finally, the results of both models are assessed using the quality index for regions of synchronized flow and wide moving jam. Figure 19 shows the results for the ASDA and FOTO models, while Figure 20 shows the results for

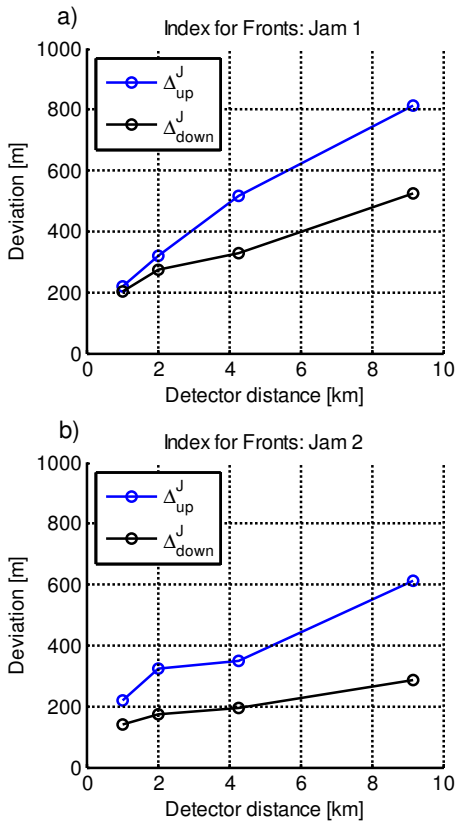

Figure 15. Quality Index for Fronts (Deviation): ASDA and FOTO

the models based on probe vehicle data. Again the models based on probe vehicle data are superior to the ASDA and FOTO models. At an equipment rate of about 1-1.5 % the results are comparable to a dense detector network with an average detector distance of 1 km. In addition the false alarm rates are very low for all examined equipment rates. In comparison the models ASDA and FOTO show an increasing false alarm rate as the detector distance increases.

In addition the results of both models can be compared directly, when both of them are plotted as a ROC curve in the ROC space. In this case TPR is plotted over FPR. A random decision is represented by the line $TPR = FPR$. All results above this line are better than the random decision, all results below this line are worse than the random decision. The maximum quality in the ROC space is represented by the point $TPR = 1$ and $FPR = 0$. Figure 21 shows the results of both models in the ROC space. These results underline the previously discussed results. The probe vehicle based methods offer higher hit rates combined with lower false alarm rate. This leads to an overall better quality. The reconstruction quality is much better for the traffic phase J when compared to the traffic phase S. The reason for this is the stable upstream propagation of the traffic phase J, which allows a high quality prediction of the future movement of the traffic phase and thus a high quality reconstruction of

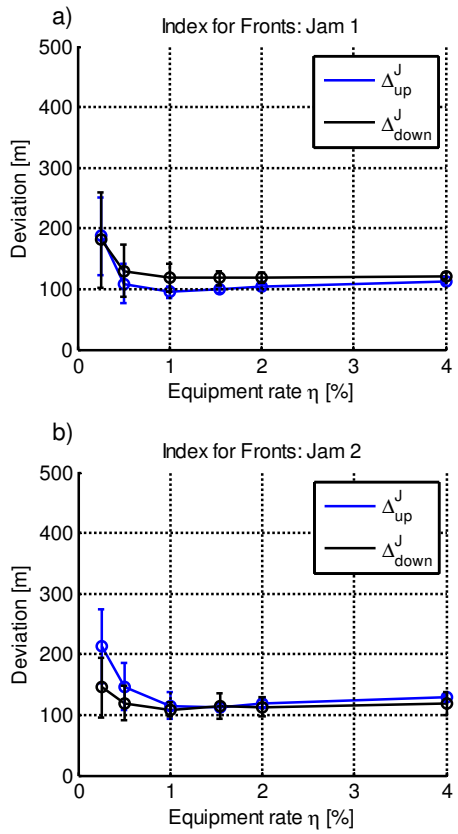

Figure 16. Quality Index for Fronts (Deviation): Vehicles

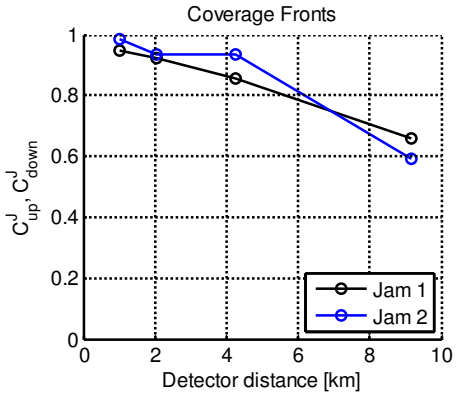

Figure 17. Quality Index for Fronts (Coverage): ASDA and FOTO

the overall region by a model.

E. Application for Empirical Data of Moving Probe Vehicles

The results shown above have been achieved using simulated traffic data. A cooperation with TomTom gave the authors the opportunity to check the methods and results with real-world data from a chosen traffic situation [21]. This real traffic situation is a congested situation on the freeway A5 in Germany on the 10th December, 2009. The situation is similar to the simulated example from Figure 10.

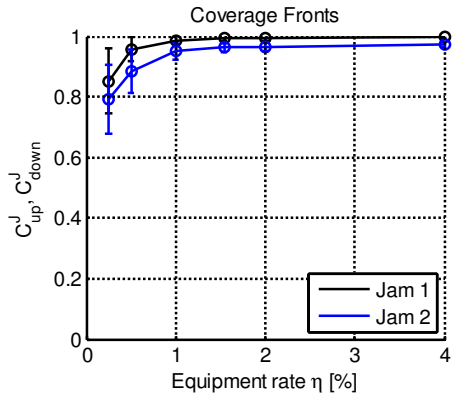

Figure 18. Quality Index for Fronts (Coverage): Vehicles

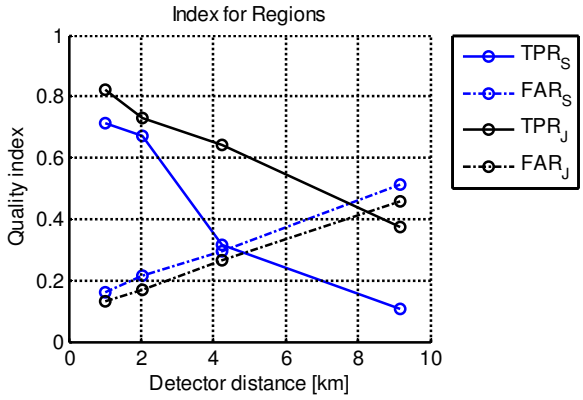

Figure 19. Quality Index for Regions: ASDA and FOTO

The number of probe vehicles collecting data for TomTom reach an equipment rate of approximately $\eta \approx 1\%$ for this traffic situation. Figure 22 a) illustrates the results after processing the TomTom probe vehicle data with the traffic state detection algorithm, while Figure 22 b) shows the results of the phase front detection. In Figure 22 c) consequently the overall spatial-temporal reconstructed congested pattern

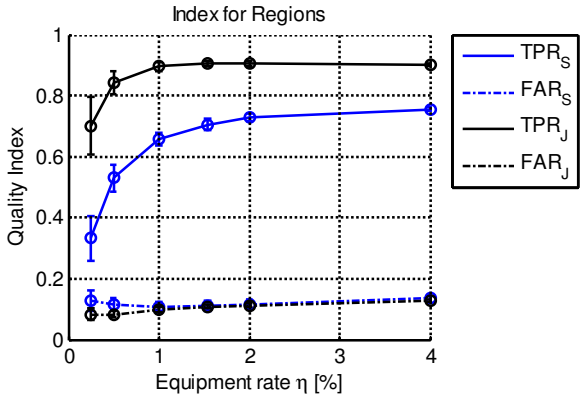

Figure 20. Quality Index for Regions: Vehicles

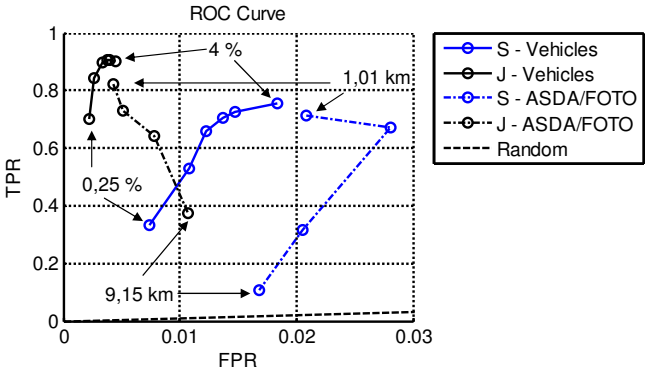

Figure 21. Quality Index for Regions: ROC Curve

based on real probe vehicle data is presented.

The following Figure 23 presents an empirical comparison for the same traffic situation based on different measurement techniques and data processing methods. At the top the results of the ASDA and FOTO models for the measured detector data and at the bottom the congested pattern based on TomTom probe vehicle data and reconstructed with vehicle based methods. The results prove that based on an equipment rate of approximately $\eta \approx 1\%$ the possible data reconstruction quality is in the order of the ASDA and FOTO models for average detector distances of ≈ 1 km.

Qualitatively a good correlation of both congested traffic phase regions *S* and *J* can be identified. Between the positions 0 km and 5 km the pattern reconstructed from probe vehicle data (Figure 23 b)) shows smaller regions of the traffic phase *S*, which do not exist in the ASDA and FOTO reconstructed pattern (Figure 23 a)). At the location between 0-5 km the detectors are more sparse than at other sections of the freeway and the traffic phase *S*, therefore, can be detected and reconstructed less precise in the ASDA and FOTO models. Those congested regions can been identified only with probe vehicle data based reconstruction methods. Overall, in this real-world case study the processing of *different* raw traffic data sources with *different* reconstruction methods has led to *comparable* results.

VIII. Conclusion and Future Work

Probe vehicle equipment rates of about 1-1.5 % processed with the proposed method are comparable to detectors with distances of 1-2 km processed with the existing ASDA and FOTO models. In addition, the proposed method promises the provision of high quality traffic data on all highways while existing systems rely on stationary loop detectors. Higher probe vehicle equipment rates promise an even higher quality traffic data suitable for future ITS and vehicular assistance applications. It should be noted, that this 1-1.5 % of vehicle data has been processed optimally, i.e., without data failures and without additional latencies of communication channels. A real-world case of traffic

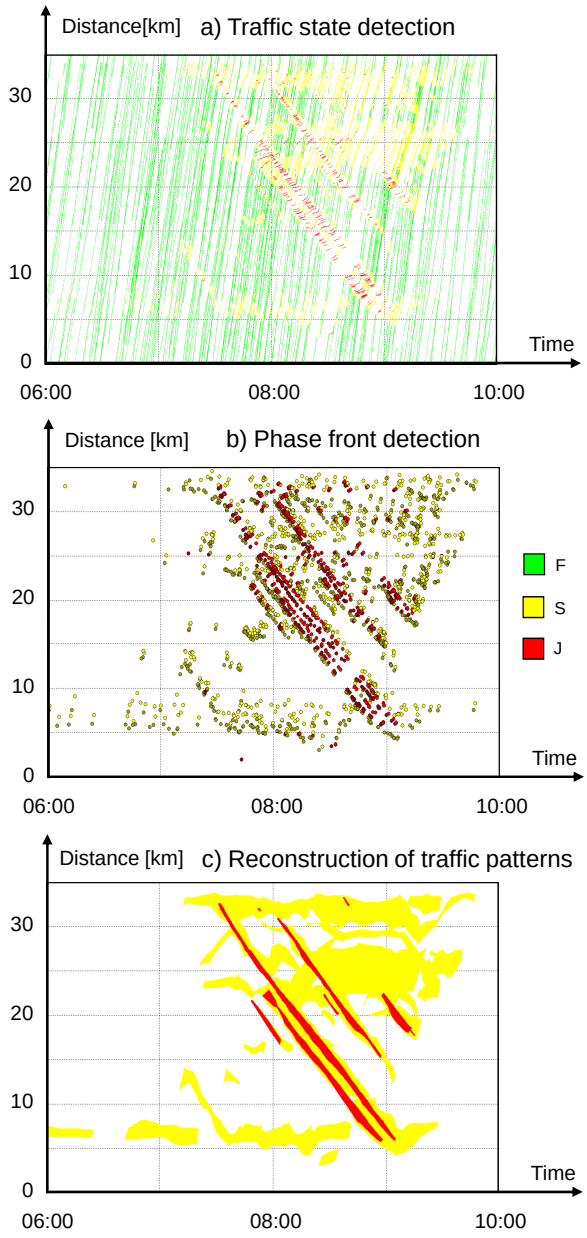

Figure 22. Reconstruction based on TomTom's probe vehicle data on 10th December, 2009 on the A5-South in Hessen, Germany [13]

congestion has proven that the processing of *different* raw traffic data (detectors and probe vehicles) have led with *different* methods (ASDA and FOTO models and probe data processing) to *comparable* results.

Subjects of further ongoing research are the evaluation and prototyping of new vehicular assistance applications based on high quality information about traffic patterns. Different types of vehicular assistance applications benefit from different parts of information about congested traffic patterns. For example having good results in the quality

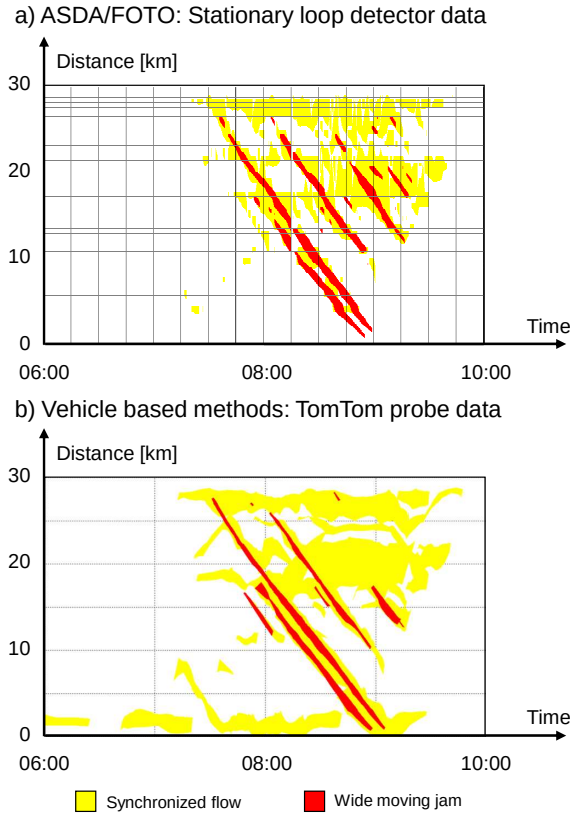

Figure 23. Traffic congestion on 10th December, 2009 at A5-South - Comparison of different reconstruction results for different empirical measurements [13]

index of travel time is relevant for routing applications, while applications controlling an hybrid engine would benefit from good results in the quality index for fronts of synchronized flow and wide moving jam. Future research has to answer the important question about the performance of specific vehicular assistance applications on the reconstruction quality of congested traffic patterns. This might include the definition of additional quality indices, which are tailored to the requirements of specific vehicular assistance applications. For example the reconstruction quality of traffic state changes from F to J could be more important to some applications than traffic state changes from F to S. An additional quality could take these differences into account.

Another relevant field for future research is the evaluation of system communication and system architecture alternatives. Different system architectures, like for example central server based systems and fully distributed systems using only communicating vehicles, have different advantages and disadvantages, when it comes to the overall system performance in comparison to the investment needed to establish and maintain these system architectures.

ACKNOWLEDGMENT

The authors would like to thank Boris S. Kerner and Sergey L. Klenov for support regarding the microscopic three-phase traffic model, the simulated vehicle data, and many fruitful discussions. In addition, we would like to thank Ralf-Peter Schaefer and Nikolaus Witte from TomTom for their support with evaluating probe vehicle data.

REFERENCES

[1] K. Bogenberger, *Qualitaet von Verkehrsinformationen* Strassenverkehrstechnik, Kirschbaum Verlag GmbH Bonn, pp. 10:518–526, 2003.

[2] D. Ehmanns, H. Wallentowitz, C. Gelau, and F. Nicklisch, *Zukuenftige Entwicklungen von Fahrerassistenzsystemen und Methoden zu deren Bewertung* In Proceedings: 9. Aachener Kolloquium Fahrzeug- und Motorentechnik, 2000.

[3] T. Fawcett, *ROC graphs: Notes and practical considerations for researchers* Machine Learning, pp. 1–38, 2004.

[4] J.C. Herrera, D.B. Work, R. Herring, X.J. Ban, Q. Jacobson, and A.M. Bayen, *Evaluation of traffic data obtained via GPS-enabled mobile phones: The Mobile Century field experiment* TTransportation Research Part C: Emerging Technologies, pp. 2:135–166, 2008.

[5] B.S. Kerner, *The Physics of Traffic* Berlin, New York: Springer, 2004.

[6] B.S. Kerner, S. L. Klenov, J. Palmer, M. Prinn, and H. Rehborn, *Verfahren zur Verkehrszustandsbestimmung in einem Fahrzeug* German Patent Publication DE 10 2008 003 039, 2008.

[7] B.S. Kerner, *Betriebsverfahren fuer ein in einem Fahrzeug befindliches verkehrsadaptives Assistenzsystem* German Patent Publication DE 10 2005 017 560, 2005.

[8] B.S. Kerner, *Introduction to Modern Traffic Flow Theory and Control* Berlin, New York: Springer, 2009.

[9] B.S. Kerner, H. Rehborn, M. Aleksic, A. Haug, and R. Lange, *Online automatic tracing and forecasting of traffic patterns* Traffic Engineering & Control, Hemming, pp. 10:345–350, 2001.

[10] B.S. Kerner, H. Rehborn, J. Palmer, and S.L. Klenov, *Using probe vehicle data to generate jam warning messages* Traffic Engineering & Control, Hemming, pp. 3:141–148, 2011.

[11] A. Kesting, *Microscopic Modeling of Human and Automated Driving: Towards Traffic-Adaptive Cruise Control* PhD Thesis, Technical University of Dresden, 2008.

[12] S. Lorkowski, *Fusion von Verkehrsdaten mit Mikromodellen am Beispiel von Autobahnen* PhD Thesis, Technical University of Berlin, 2009.

[13] J. Palmer, *Fahrzeugautonome und verteilte Erkennung rauemlich-zeitlicher Verkehrsmuster zur Nutzung in Fahrerassistenzsystemen* PhD Thesis, University of Tuebingen, 2011.

[14] J. Palmer and H. Rehborn, *Reconstruction of Congested Traffic Patterns Using Traffic State Detection in Autonomous Vehicles Based on Kerner's Three Phase Traffic Theory* In Proceedings: 16th World Congress on ITS, Stockholm, 2009.

[15] J. Palmer and H. Rehborn, *Vehicular Assistance Applications in the Scope of Kerner's Three-Phase Traffic Theory* In Proceedings: Networks for Mobility - 5th International Symposium, Stuttgart, 2010.

[16] J. Palmer and H. Rehborn, *Reconstruction Quality of Congested Freeway Traffic Patterns from Probe Vehicles Based on Kerner's Three-Phase Traffic Theory* In Proceedings: 6th International Conference on Systems - ICONS, St. Maarten, The Netherlands Antilles, 2011.

[17] J. Palmer, H. Rehborn, and B.S. Kerner, *ASDA and FOTO Models based on Probe Vehicle Data* Traffic Engineering & Control, Hemming, pp. 4:183–191, 2011.

[18] H. Rehborn and J. Palmer, *ASDA/FOTO based on Kerner's Three-Phase Traffic Theory in North Rhine-Westphalia and its Integration into Vehicles* In Proceedings: 2008 IEEE Intelligent Vehicles Symposium, Eindhoven, 2008.

[19] H. Rehborn, S. L. Klenov, and J. Palmer, *An empirical study of common traffic congestion features based on traffic data measured in the USA, the UK, and Germany* Physica A 390, pp. 4466-4485, 2011.

[20] H. Rehborn and S. L. Klenov, *Congested Traffic Prediction of Congested patterns* In: Meyers, Robert (Ed.) Encyclopedia of Complexity and Systems Science, Springer New York, pp. 9500-9536, 2009.

[21] R.-P. Schaefer, S. Lorkowski, N. Witte, J. Palmer, H. Rehborn, and B.S. Kerner, *A study of TomToms probe vehicle data with three phase traffic theory* Traffic Engineering & Control, Hemming, pp. 5:225–230, 2011.

[22] M. Schoenhof and D. Helbing, *Empirical Features of Congested Traffic States and Their Implications for Traffic Modeling* Transportation Science, pp. 4:568–583, 2010.

[23] J.A. Sweets, *Measuring the Accuracy of Diagnostic Systems,* Science, 240(4857), pp. 1285–1293, 1988.

[24] K. Veropoulos, C. Campbell, and N. Cristianini, *Controlling the Sensitivity of Support Vector Machines* In Proceedings: IJCAI - International Joint Conference on Artificial Intelligence, Workshop on Support Vector Machines, Stockholm, Schweden, 1999.